International Journal of Rock Mechanics & Mining Sciences 57 (2013) 167–171

Contents lists available at SciVerse ScienceDirect

International Journal of
Rock Mechanics & Mining Sciences

journal homepage: www.elsevier.com/locate/ijrmms

Laboratory testing of steel fibre reinforced shotcrete

H. Saw*, E. Villaescusa, C.R. Windsor, A.G. Thompson

CRC Mining, Western Australian School of Mines, Curtin University, PMB 30, Kalgoorlie 6430, Australia

ARTICLE INFO

Article history:
Received 15 July 2011
Received in revised form
22 March 2012
Accepted 19 August 2012
Available online 5 November 2012

Keywords:
Uniaxial and triaxial compression tests
Steel fibre reinforced shotcrete
Elastic and plastic mechanical properties

ABSTRACT

Uniaxial and triaxial compression tests on steel fibre reinforced shotcrete (SFRS) have been used to quantify the elastic–plastic response behaviour for both the peak and post-peak regions. The laboratory tests were conducted with a servo-controlled testing machine to obtain complete stress–strain curves. The test results include unconfined and triaxial compressive strengths, shear strengths and tensile strengths together with the elastic and plastic mechanical properties of SFRS. A method is also suggested for obtaining the plasticity parameters for non-linear modelling of SFRS.

1. Introduction

The theory of plasticity is the name given to the mathematical study of stress and strain in plastically deformed solids [1]. Hill published the book "Mathematical theory of plasticity" based mainly on the test results of metals. However, he did suggest that the theory may apply to other potentially plastic materials. Since that time, extensive research and development has been conducted on the application of plasticity theory to materials such as soils, rocks, concrete and shotcrete. To date, the theory has reached a good degree of maturity for application to geomaterials, although further progress is still expected [2]. At the same time the continual development of testing equipment, computing methods, software and hardware enhance the application of plasticity theory.

Shotcrete is a designed material with anisotropic, inhomogeneous and elastic–plastic behaviour. Therefore, understanding of the complete stress–strain behaviour of shotcrete is extremely important in ground support design, especially in cases where large deformations are expected such as around mine excavations at great depth. A rock mass is naturally Discontinuous, Inhomogeneous, Anisotropic, and Non-Elastic (DIANE) [3]. When a rock mass deforms non-linearly, the shotcrete also responds non-linearly. Deformation mechanisms of shotcrete which support the rock mass surface excavated by drill and blast methods are described by Windsor and Thompson [4].

2. Literature review and objectives of this study

Tejchman and Kozicki [5] reviewed the works of different researches on the steel fibre reinforced concrete and summarised the most important physical and mechanical properties of steel fibre reinforced concrete/shotcrete. Most of the experiments were concerned with the influences of constituent materials such as the types and dosages of fibre, cement, aggregate, additives and admixtures on the physical and mechanical properties of steel fibre reinforced concrete/shotcrete. The literature shows that the most common tests are uniaxial compressive strength (UCS), beam flexural strength and panel toughness and energy absorption test e.g. [6]. Many parameters are required for non-linear, elastic–plastic numerical modelling for the rock mass and rock improvement system (i.e. rock bolts, shotcrete and wire mesh). The fundamental material parameters include Young's modulus, Poisson's ratio, uniaxial compressive strength (UCS), shear strength (both peak and residual cohesion (c) and friction (ϕ)), tensile strength, dilation angle (ψ) and strain rate at peak and residual strength. In addition, geological conditions such as major and minor structures, stresses and hydrology need to be taken into account.

The main objectives of this study are to quantify elastic–plastic response behaviour of shotcrete for both the peak and post-peak regions under uniaxial and triaxial loading, to predict the shear strength in terms of cohesion (c), friction (ϕ) and dilation angles (ψ) and, to examine how these parameters vary with curing time. The laboratory test results are presented as simple stress–strain curves from which the parameters were derived.

3. A complete stress–strain relation

In the elastic region the strains are linearly related to the stress as assumed in Hooke's Law [7]. In the elastic region strains are uniquely determined by stresses and can be computed directly using Hooke's law without any regard to how the stress state was

* Corresponding author. Tel.: +61 8 90886099; fax: +61 8 90886151.
E-mail address: h.saw@curtin.edu.au (H. Saw).

1365-1609/$ - see front matter © 2012 Elsevier Ltd. All rights reserved.
http://dx.doi.org/10.1016/j.ijrmms.2012.08.008

attained. Mathematically, elastic strain (ε^e) and stress (σ) can be related simply as

$$\varepsilon^e = \frac{\sigma}{E} \tag{1}$$

where E is Young's modulus.

In the plastic region, the strains are not uniquely determined by the stresses but depend on the whole history of loading or how the stress state was reached. An essential part of plasticity theory is to define when the material starts to deform or yield. A failure criterion is used to describe the point at which fracture or yield occurs. The criterion under which yield occurs is called a yield criterion. The most widely used yield criterion is the Coulomb yield criterion [8].

$$\tau = c + \sigma_n \tan\phi \tag{2}$$

where τ and σ_n represent the shear stress and normal stress, respectively. Compressive stress components are treated as positive, as is usual in geomechanics. The parameters c and ϕ are assumed to be constants. However, c and ϕ change with stress level. Once the yield criterion is satisfied, the material will flow obeying a flow rule. The flow rule is termed associated if the plastic strains are related directly with the yield surface and, if not, it is termed non-associated. The non-associated flow rule states that the plastic strain rate is proportional to the derivatives of the plastic potential with respect to the corresponding stress. This can be described by the following equation:

$$\delta\varepsilon^p = \lambda \frac{\partial g}{\partial \sigma} \tag{3}$$

where $\delta\varepsilon^p$ is the plastic strain increment, λ is the Lagrange or plastic multiplier, and g is a plastic potential. The definition of the plastic potential function "g" suggested by Radenkovic [9] is

$$g = \tau + \sigma \sin\psi + \text{constant} \tag{4}$$

where ψ is the dilation angle. Hansen suggested that a dilation angle is defined as the ratio of plastic volume change divided by plastic shear strain [10].

For the Mohr–Coulomb yield criterion, Eq. (4) can be written in terms of principal stresses for triaxial test conditions where, $\sigma_2 = \sigma_3$

$$g = \frac{1}{2}(\sigma_1 - \sigma_3) + \frac{1}{2}(\sigma_1 + \sigma_3)\sin\psi + \text{constant} \tag{5}$$

The principal plastic strain rates are obtained by differentiating Eq. (5) with respect to the principal stresses as given in Eq. (3):

$$\begin{bmatrix} \delta\varepsilon_1^p \\ \delta\varepsilon_2^p \\ \delta\varepsilon_3^p \end{bmatrix} = \lambda \begin{bmatrix} \frac{1}{2}(1+\sin\psi) \\ \frac{1}{2}(-1+\sin\psi) \\ \frac{1}{2}(-1+\sin\psi) \end{bmatrix} \tag{6}$$

where $\{\delta\varepsilon_1^p, \delta\varepsilon_2^p, \delta\varepsilon_3^p\}$ are the major, intermediate and minor plastic strain increments, respectively. It follows that

$$\delta\varepsilon_v^p = \lambda \sin\psi \tag{7}$$

$$\delta\varepsilon_1^p = \frac{1}{2}\lambda(1+\sin\psi) \tag{8}$$

where the volumetric strain increment $\delta\varepsilon_v^p$ is the sum of $\{\delta\varepsilon_1^p, \delta\varepsilon_2^p, \delta\varepsilon_3^p\}$.

By eliminating λ from Eqs. (7) and (8), $\sin\psi$ is given by

$$\sin\psi = \frac{\delta\varepsilon_v^p}{2\delta\varepsilon_1^p + \delta\varepsilon_v^p} \tag{9}$$

This equation for $\sin\psi$ may also be expressed as

$$\sin\psi = \frac{1}{(2\delta\varepsilon_1^p/\delta\varepsilon_v^p) + 1} \tag{10}$$

The ratio $\delta\varepsilon_v^p/\delta\varepsilon_1^p$ is equivalent to the slope of volumetric–axial strain curve. Therefore, the inverse of the slope can be substituted into Eq. (11) to obtain the dilation angle ψ.

A plastic strain (ε^p), found by subtracting the elastic strain from the total strain, may written as

$$\varepsilon^p = \varepsilon^t - \varepsilon^e \tag{11}$$

4. Experimental programme

4.1. Mix design and curing method

The wet mix shotcrete used in these investigations is similar to that used at one of underground gold mines in the Eastern Gold Fields region of Kalgoorlie, Western Australia. Shotcrete panels were sprayed on site and delivered to the WASM geomechanics laboratory on the same day. Cylindrical specimens were cored from the panels and stored in a curing chamber, which was set at 30 °C and 90% humidity. The tests were conducted on batches of three samples after four different curing periods (1, 3, 7 and 28 days). All of the shotcrete batches have the same mix design which is given in Table 1.

4.2. Test method

Both uniaxial and triaxial compressive tests were conducted according to the methods suggested by the International Society of Rock Mechanics (ISRM) [11–13]. These tests were performed using an Instron, servo-controlled hydraulic testing machine. The displacement rate of the machine was set at 0.12 mm/min. The strains were measured with two, biaxial foil strain gauge with 10 mm gauge lengths that were installed diametrically opposite at the specimen mid-height. The triaxial compression test is a useful test method to obtain a complete stress–strain response of the SFRS sample and to derive the shear strength parameters and dilation angles. Three different confining pressures 1, 2 and 3 MPa were applied to the three specimens within each batch. The tensile strength was obtained according to the test method suggested by ISRM [14] known as the Brazilian test. The test was performed with an Avery universal testing machine. Load and displacement were monitored and stored at resolutions of 0.01 kN and 0.02 mm, respectively.

5. Results and discussion

5.1. Uniaxial compressive strength test results

The stress–strain curves are shown in Fig. 1. The parameters derived from these test results are summarised in Table 2. The test results show that UCS increases with curing time and that

Table 1
Mix design of SFRS used in this research.

Material	Quantity for 1 m^3 mix
Cement (general purpose)	440 kg
Coarse aggregate ($_{Max}$. 7 mm)	220 kg
Crusher dust	1300 kg
Sand	1640 kg
Water	150 L
Steel fibres (Dramix)	30 L
Liquid Meyco (MS 685)	11 L
Delvo Stabiliser	5 L
Rheobuild 1000	8 L
Pozzolith 322NI	1.3 L
Accelerator	4% of cement

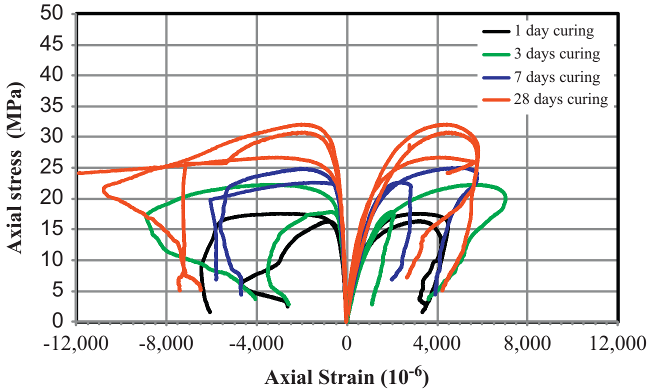

Fig. 1. Stress versus strain curves from UCS test.

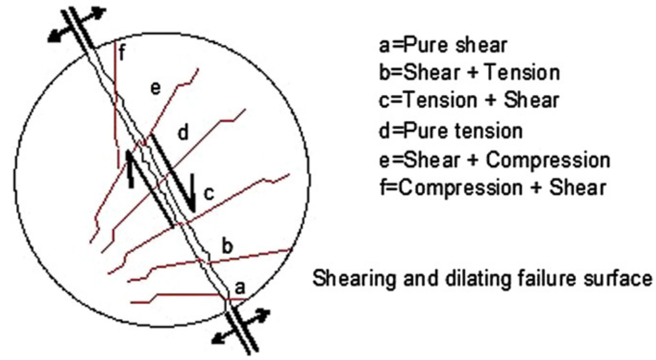

Fig. 2. Effective fibre with various response modes for different fibre orientations. (Modified from Windsor [15]).

Table 2
Summary of UCS test with complete stress–strain measurement.

Batch no.	Curing (days)	Unit weight (kN/m^3)	UCS, σ_c (MPa)	Elastic properties					
				Young's modulus			Poisson's ratio		
				E_{t50} (GPa)	E_s (GPa)	E_a (GPa)	ν_{t50}	ν_s	ν_a
1	1	20.71	16.2	–	–	–	–	–	–
2	1	20.71	18.1	14	15	14	0.36	0.31	0.42
3	1	23.44	18.3	11	16	11	0.20	0.28	0.19
1	3	23.44	23.4	–	–	–	–	–	–
2	3	22.75	18.3	12	15	12	0.28	0.29	0.28
3	3	23.39	22.9	9	13	8	0.16	0.21	0.16
1	7	23.54	28.5	–	–	–	–	–	–
2	7	23.48	23.2	16	21	16	0.23	0.34	0.22
3	7	23.57	25.7	14	17	14	0.17	0.29	0.17
1	28	23.44	32.8	15	21	14	0.21	0.31	0.21
2	28	23.68	27.2	18	28	17	0.30	0.29	0.29
	28	23.05	31.5	11	16	10	0.17	0.22	0.15

Note: E_{t50}, Tangent Young's modulus; E_s, Secant Young's modulus; E_a, Average Young's modulus; ν_{t50}, Tangent Poisson's ratio; ν_s, Secant Poisson's ratio; ν_a, Average Poisson's ratio.

Young's modulus and Poisson's ratio do not change significantly. The yield point of the curves increased with increasing UCS. After yield, non-linear strain hardening can be observed until the stress reaches a peak. After peak, localised damage develops and strain softening and/or the "snap-back" begins. The "snap-back" implies that the materials failed in a brittle mode. Globally, the SFRS continued to deform in shear associated with dilation with the load taken by steel fibres. The effective steel fibres are those which span the failure surface and are firmly anchored on both sides. The post peak behaviour of SFRS is highly dependent on the numbers and orientations of the effective fibres. Fig. 2 shows that steel fibres with various orientations respond in different modes. The responses are predominantly shear, tensile and compression in nature. The most common response is a combination of these modes.

5.2. Brazilian indirect tensile strength test results

Fig. 3 shows the load–displacement curves for indirect tensile strength tests. The summary of Brazilian test results is given in Table 3. Similar to the UCS tests, the tensile strength also increases with curing age. The results suggest that, after first crack, the load is taken by the effective fibres and the ultimate tensile strength depends on the numbers and orientation of the effective fibres. Fig. 4 shows the correlation between the UCS and the peak tensile strength. The correlation suggests that the peak tensile (Brazilian) strength of SFRS is about 15% of its UCS.

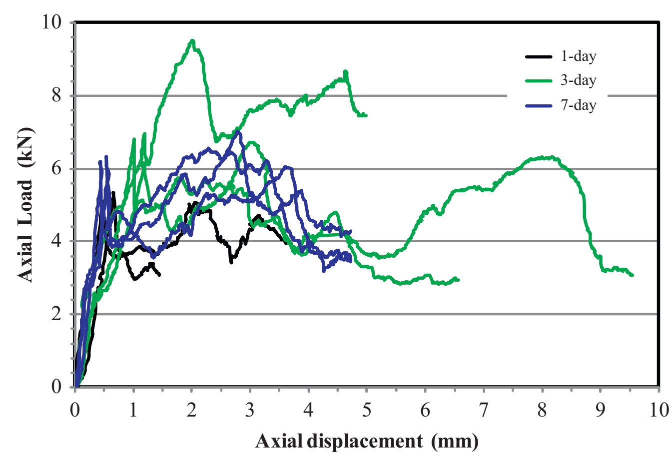

Fig. 3. Load–displacement curves from Brazilain tests.

Table 3
Summary of Brazilian test results.

Batch no.	Curing (days)	Peak tensile strength (MPa)
3	1	2.4
3	1	2.5
2	3	3.4
3	3	2.8
3	3	4.3
3	3	3.5
2	7	4.4
2	7	4.0
3	7	3.6
3	7	2.8
3	7	3.2
1	28	5.5
1	28	4.0
2	28	4.9
3	28	5.4
3	28	5.1
3	28	4.8

5.3. Triaxial test results

A summary of test results is given in Table 4. The shear strength parameters presented in Table 4 are calculated based

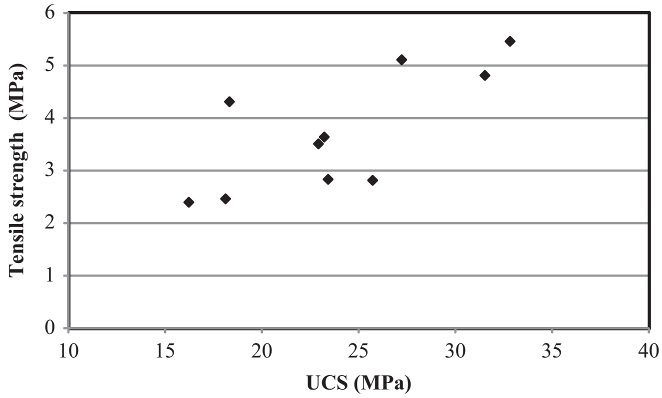

Fig. 4. Correlation of peak tensile strength and UCS.

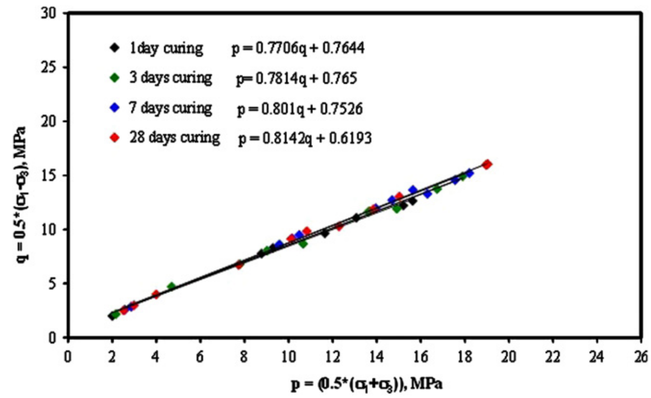

Fig. 6. Residual shear strength envelopes plotted on the p–q plane.

Table 4
Summary of Triaxial test results.

Batch no.	Curing (days)	Shear strength				Dilation angle (ψ)
		Peak		Residual		
		c (MPa)	$\phi°$	c (MPa)	$\phi°$	
1	1	4	38	–	–	–
2	1	4	45	2	45	8
3	1	5	36	5	32	13
1	3	5	40	3	42	–
2	3	4	40	3	41	10
3	3	6	38	–	–	12
1	7	8	35	5	35	–
2	7	5	40	4	41	10
3	7	6	40	5	38	10
1	28	8	38	7	18	12
2	28	11	18	–	–	12
3	28	8	38	–	–	10

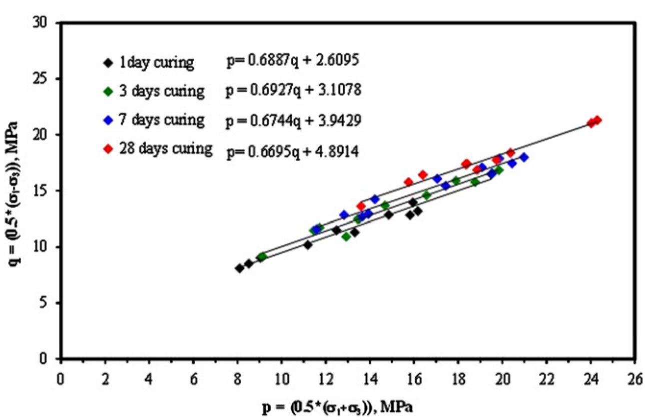

Fig. 5. Peak shear strength envelopes plotted on the p–q plane.

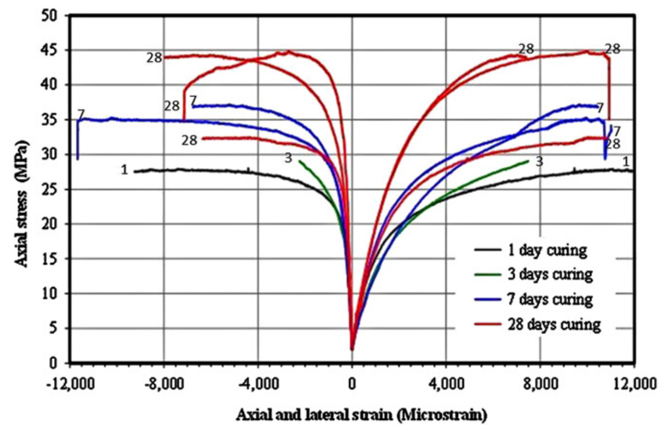

Fig. 7. Axial stress versus strain curves at 3 MPa confinement.

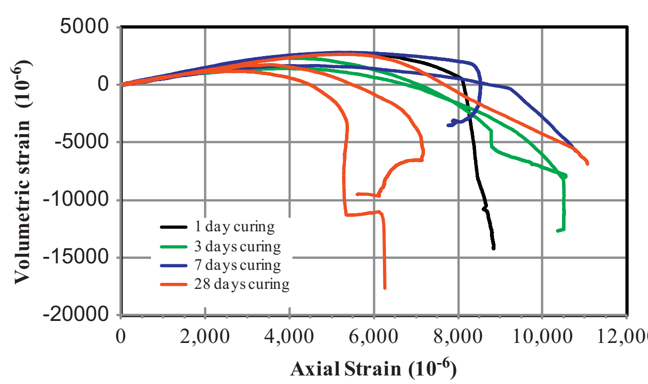

Fig. 8. Axial strain versus volumetric curves at 1 MPa confinement.

on Coulomb's failure theory [7,12]. Alternatively, the peak and residual strength envelopes plotted on the p–q plane are also shown in Figs. 5 and 6 respectively. Generally, the shear strength increased with curing time. The friction and dilation angles do not change significantly with curing time. The residual strength is influenced by confining pressure. The main cause of increase in strength is an increase in cohesion, with the slopes of the lines associated with friction angle being very similar.

The plastic strain Eq. (11) can be used to calculate the plastic strain rate at peak and residual stress using the stress–strain curves shown in Fig. 7. The plastic strain increased with increasing confining pressure. The peak stress does not change significantly from 1 day to 7 day curing but significantly increased after 28 days. The dilation angles are calculated from the axial and volumetric strain curves as described in Section 3. Fig. 8 shows the axial and volumetric strain curves at 1 MPa confinement. The correlation of friction and dilation angles is shown in Fig. 9. This suggests that higher dilations occurred in samples with lower friction angles. Also, the amount of dilation decreased with increasing confining pressure.

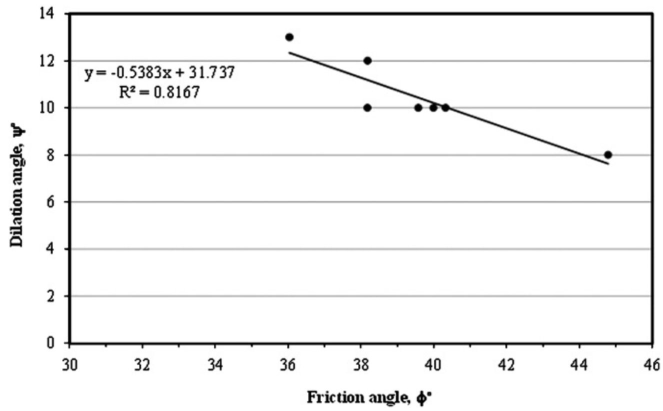

Fig. 9. Correlation between the friction angle and the dilation angle.

6. Concluding remarks

A test programme was conducted on steel fibre reinforced shotcrete (SFRS) samples to define the mechanical parameters for non-linear, elastic–plastic modelling. In particular, uniaxial and triaxial compression tests and Brazilian tests were used to quantify elastic–plastic response behaviours for both the pre-peak and post-peak regions. The findings suggest that the residual strength is influenced by the confining pressure as the specimen responded to continuously strain hardening after post peak. The dilation angle ranges from 8 to 13 degrees and does not change significantly with curing time. It decreases with increasing friction angle. The amount of dilation decreases with increasing confining pressure. A complete stress–strain response can be subdivided into linear elastic and non-linear plastic regions. The post peak behaviour is influenced by the confining pressure and the number and orientation of effective fibres.

Acknowledgements

The writers wish to thank Barrick Gold of Australia Limited for their funding and for supplying the steel fibre reinforced shotcrete slabs.

References

[1] Hill R. The mathematical theory of plasticity. Oxford: Oxford University Press; 1950.
[2] Yu HS. Plasticity and geotechnics. New York: Springer; 2006.
[3] Harrison JP, Hudson JA. Engineering rock mechanics, part 2. Oxford: Elsevier; 2000.
[4] Windsor CR, Thompson AG. The design of shotcrete linings for excavations created by drill and blast methods. In: Proceedings of international symposium on ground support, Kalgoorlie; 1999. p. 231–41.
[5] Tejchman J, Kozicki J. Experimental and theoretical investigation of steel-fibrous concrete. Berlin: Springer; 2010.
[6] Morgan DR, Mowat DN. A comparative evaluation of plain, mesh and steel fibre reinforced concrete. In: Morgan DR, editor. Shotcrete—a compilation of papers. Farmington Hill: American Shotcrete Association; 2008. p. 95–112.
[7] Hooke R. The posthumous works, containing his Cutlerian lectures, and other discourses. Read at the Meeting of the Illustrious Royal Society; 1705.
[8] Coulomb CA. Essais sur une application des regles des maximis et minimis à quelques problems de statique relatifs à l'architecture. Mém. Acad. Roy. Des Sciences, Paris, 1776:343–82.
[9] Radenkovic D. Théorèmes limites pour un matériau de Coulomb á dilation non standardisée. CR Acad Sci 1961;252:4103–4.
[10] Hansen CEB. Line ruptures regarded as narrow rupture zones—basic equations based on kinematic considerations. In: Proceedings of the conference on Earth pressure problem, Brussels; 1958.
[11] ISRM. Suggested methods for determining the uniaxial compressive strength and deformability of rock material. In: Brown ET, editor. Rock characterization, testing and monitoring: ISRM suggested methods. Oxford: Pergamon; 1981. p. 137–40.
[12] Fairhurst CE, Hudson JA, Draft ISRM. Suggested method for the complete stress–strain curve for intact rock in uniaxial compression. Int J Rock Mech Min Sci 1999;36:279–89.
[13] ISRM. Suggested methods for determining the strength of rock materials in triaxial compression: revised version. Int J Rock Mech Min Sci 1983;20:285–90.
[14] ISRM. Suggested methods for determining tensile strength of rock mateials. Int J Rock Mech Min Sci 1978;15:90–103.
[15] Windsor CR. Rock reinforcement systems. Int J Rock Mech Min Sci. Geomech 1996;34(6):919–51.